A systematic examination of the relationships between CDOM and DOC in inland waters in China

Kaishan Song[1], Ying Zhao[1, 2], Zhidan Wen[1], Chong Fang[1, 2], Yingxin Shang[1]

[1]Northeast Institute of Geography and Agroecology, CAS, Changchun, 130102, China

[2] University of Chinese Academy of Sciences, Beijing 100049, China

Corresponding author's E-mail: songks@iga.ac.cn; Tel: 86-431-85542364

Abstract: Chromophoric dissolved organic matter (CDOM) plays a vital role in the biogeochemical cycle in aquatic ecosystems. The relationship between CDOM and dissolved organic carbon (DOC) has been investigated, and the significant relationship lays the foundation for the estimation of DOC using remotely sensed imagery data. The current study examined the samples from freshwater lakes, saline lakes, rivers and streams, urban water bodies, and ice-covered lakes in China for tracking the variation of the relationships between DOC and CDOM. The regression model slopes for DOC versus $a_{CDOM}(275)$ ranged from extreme low 0.33 (highly saline lakes) to 1.03 (urban waters) and 3.01 (river waters). The low values were observed in saline lake waters and waters from semi-arid or arid regions where strong photo-bleaching is expected due to less cloud cover, longer water residence time and daylight hours. In contrast, high values were found in waters developed in wetlands or forest in Northeast China, where more organic matter was transported from catchment to waters. The study also demonstrated that closer relationships between CDOM and DOC were revealed when $a_{CDOM}(275)$ were sorted by the ratio of $a_{CDOM}(250)/a_{CDOM}(365)$, which is a measure for the CDOM absorption with respect to its composition, and the determination of coefficient of the regression models ranged from 0.79 to 0.98 for different groups of waters. Our results indicated the relationships between CDOM and DOC are variable for different inland waters, thus models for DOC estimation through linking with CDOM absorption need to be tailored according to water types.

Keywords: Absorption, CDOM, DOC, regression slope, saline water, fresh water

1. Introduction

Inland waters play a disproportional role for the global carbon cycling with respect to carbon transportation, transformation and carbon storage (Tranvik et al., 2009; Raymond et al., 2013; Verpoorter et al., 2014; Yang et al., 2015). However, the amount of dissolved organic carbon (DOC) stored in the inland waters is still unclear or the uncertainty is still needed to be evaluated (Tranvik et al., 2009). Determination DOC concentration is straightforward through field sampling and laboratory analysis (Findlay and Sinsabaugh, 2003). However, there are millions of lakes in the world, and many of them are remote and inaccessible, making it impossible to evaluate DOC concentration using routine approach (Cardille et al., 2013; Brezonik et al., 2015; Pekel et al., 2016). Researchers have found that remote sensing might provide a promising tool for quantification of DOC of inland waters at large scale through linking DOC with chromophoric dissolved organic matter (CDOM), particularly for inland waters situating in remote area with less accessibility (Tranvik et al., 2009; Kutser et al., 2015; Brezonik et al., 2015).

As one of the optically active constituents (OACs) in waters, CDOM can be estimated through remotely sensed signals (Yu et al., 2010; Kutser et al., 2015), and is acted as a proxy in many regions for the amount of DOC in the water column. As shown in Fig.1, CDOM and DOC in the aquatic ecosystems are mainly originated from natural external (allochthonous) and internal (autochthonous) sources, in addition to directly discharge from anthropogenic activities (Zhou et al., 2016). Generally, the autochthonous CDOM essentially originates from algae and macrophytes, and mainly consists of various compounds of low molecular weights (Findlay and Sinsabaugh, 2003; Zhang et al., 2010). While, the allochthonous CDOM is mainly derived from the surrounding terrestrial ecosystems, and it comprises a continuum of small organic molecules to highly polymeric humic substances. In terms of CDOM originating from anthropogenic sources, it contains fatty acid, amino acid and sugar, thus the composition of CDOM is more complex than that from natural systems (Zhou et al., 2016; Zhao et al., 2016a). Hydrological factors also affect the DOC and CDOM characteristic and particularly, the discharge, catchment area, land use and travel time are the important ones (Neff et al., 2006; Spencer et al., 2012).

[Insert Fig.1 about here]

CDOM is a light-absorbing constituent, which is partially responsible for the color in waters (Bricaud et al., 1981; Reche et al., 1999; Babin et al., 2003). The chemical structure and origin of CDOM can be characterized by its absorption coefficients ($a_{CDOM}(\lambda)$) and spectral slopes (De Haan and De Boer, 1987; Helms et al., 2008). Weishaar et al. (2003) has proven that the carbon specific absorption coefficient at 254 nm, e.g., $SUVA_{254}$ is a good tracer for the aromaticity of humic acid in CDOM, while the ratio of CDOM absorption at 250 to 365 nm, i.e., $a_{CDOM}(250)/a_{CDOM}(365)$, herein, M value, has been successfully used to track the variation in DOM molecular weight (De Haan and De Boer, 1987). Biodegradation and photodegradation are the major processes to determine the transformation and composition of CDOM (Findlay and Sinsabaugh, 2003; Zhang et al., 2010), which ultimately affect the relationship between DOC and CDOM (Spencer et al., 2012; Yu et al., 2016). With prolonged sunlight radiation, some of the colored fraction of CDOM is lost by the photobleaching processes (Miller et al., 1995; Zhang et al., 2010), which can be measured by the light absorbance decreasing at some specific (diagnostic) wavelength, e.g., 250, 254, 275, 295, 360 and 440 nm.

It should be noted that $a_{CDOM}(440)$ is usually used by remote sensing community due to this wavelength is overlapped with pigment absorption at 443 nm, thus reporting $a_{CDOM}(440)$ has potential to improve chlorophyll-a estimation accuracy (Lee et al., 2002).The relationship between CDOM and DOC varies since CDOM loses color while the variation of DOC concentration is almost negligible. Saline or brackish lakes in the arid or semi-arid regions are generally exposed to longer sunlight radiation, thus CDOM absorbance decreases, while DOC is accumulated due to the longer residence time (Curtis and Adams, 1995; Song et al., 2013; Wen et al., 2016). Compared to photodegradation of CDOM, the biodegradation processes by microbes are much more complicated, and extracellular enzymes are the key factors required to decompose the high-molecular-weight CDOM into low-molecular-weight substrates (Findlay and Sinsabaugh, 2003). With compositional change, the absorption feature of CDOM and its relation to DOC varies correspondingly, and the relationship between CDOM and DOC needs to be systematically examined (Gonnelli et al., 2013). In addition, the $SUVA_{254}$ and M value may be used to classify CDOM into different groups and enhance the relationship with DOC based on CDOM absorption grouping.

Some studies have investigated the spatial and seasonal variations of CDOM and DOC in ice free season in lakes, rivers and oceans (Vodacek et al., 1997; Neff et al., 2006; Stedmon et al., 2011; Brezonik et al., 2015), but less is known about saline lakes (Song et al., 2013; Wen et al., 2016). Even less is known about urban waters influenced by sewage effluent and waters with ice cover in winter (Belzile et al., 2002; Zhao et al., 2016b). A significant relationship between CDOM and DOC was observed in the Gulf of Mexico, and stable regression model was established between DOC and $a_{CDOM}(275)$ and $a_{CDOM}(295)$ (Fichot and Benner, 2011). Similar results were also found in other estuaries along a salinity gradient, for example the Baltic Sea surface water (Kowalczuk et al., 2010) and the Chesapeake Bay (Le et al., 2013). However, Chen et al. (2004) found that the relationship between CDOM and DOC was not conservative due to estuarine mixing or photo-degradation. Similar arguments were raised for Congo River and waters across mainland USA (Spencer et al., 2009, 2012). In addition, seasonal variations were observed in some studies due to the mixing of various endmembers of CDOM from different terrestrial ecosystems and internal source (Zhang et al., 2010; Spencer et al., 2012; Yu et al., 2016; Zhou et al., 2016).

As demonstrated in Fig.1, several factors influence the association between DOC and CDOM, thus the relationship between DOC and CDOM may vary with respect to their origins, photo- or bio-degradations, and hydrological features, which is worth of systematic examination. In this study, the characteristics of DOC and CDOM in different inland waters across China were examined to determine the spatial feature associated with landscape variations, hydrologic conditions and saline gradients. The objectives of this study are to: 1) examine the relationship between CDOM and DOC concentrations across a wide range of waters with various physical, chemical and biological conditions, and 2) develop a model for the relationship between DOC and CDOM based on the sorted CDOM absorption feature, e.g., the M values with aiming to improve the regression modeling accuracy.

2. Materials and Methods

The dataset is composed of five subsets of samples collected from various types of waters across China (Table 1, Fig.2), which encompassed a wide range of DOC and CDOM. The first dataset (n = 288; from early spring 2009 to late October 2014) includes samples collected in freshwater lakes and reservoirs during the growing season with various landscape types. The second dataset (n = 345; from early spring 2010 to late mid-September 2014) includes samples collected in brackish to saline water bodies. The third dataset (n =322; from early May 2012 to late July 2015) includes samples collected in rivers and streams across different basins in China. In addition, 69 samples were collected from three sections along the Songhua Rive, the Yalu and the Hunjiang River during the ice free period in 2015 to examine the impact of river flow on the relationship between DOC and CDOM (see Fig.S1 for location). The fourth dataset (n = 328; from 2011 to 2014 in the ice frozen season) includes samples collected in Northeast China in winter from both lake ice and underlying waters. The fifth dataset (n = 221; from early May 2013 to mid-October 2014) collects samples in urban water bodies, including lakes, ponds, rivers and streams, which were severely polluted by sewage effluents. City maps and Landsat imagery data acquired in 2014 or 2015 were used to delineate urban boundaries with ArcGIS 10.0 (ESRI Inc., Redlands, California, USA), and water bodies in these investigated cities constrained by urban boundaries were considered as urban water bodies. The sampling dates, water body names and locations of other types of water bodies were provided in supplementary Table S1-4.

[Insert Fig.2 about here]

2.1 Water quality determination

Water samples were collected approximately 0.5m below the water surface at each station, generally locating in the middle of water bodies. Water samples were collected in two 1 L amber HDPE bottles, and kept in coolers with ice packs in the field and kept in refrigerator at 4℃ after shipping back to the laboratory. All samples were preprocessed (e.g., filtration, pH and electrical conductivity (EC) determination) within two days in the laboratory. Water salinity was measured using DDS-307 EC meter (μS/cm) at room temperature (20±2℃) in the laboratory and converted to *in situ* salinity, expressed in practical salinity units (PSU). Water samples were filtered using Whatman cellulose acetone filter with pore size of 0.45 μm. Chlorophyll-a (Chl-a) was extracted and concentration was measured using a Shimadzu UV-2600PC spectrophotometer, the details can be found in Jeffrey and Humphrey (1975). Total suspended matter (TSM) was determined gravimetrically using pre-combusted Whatman GF/F filters with 0.7μm pore size, details can be found in Song et al. (2013). DOC concentrations were measured by high temperature combustion (HTC) with water samples filtered through 0.45 μm Whatman cellulose acetone filters (Zhao et al., 2016a). The standards for dissolved total carbon (DTC) were prepared from reagent grade potassium hydrogen phthalate in ultra-pure water, while dissolved inorganic carbon (DIC) were determined using a mixture of anhydrous sodium carbonate and sodium hydrogen carbonate. DOC was calculated by subtracting DIC from DTC, both of which were measured using a Total Organic Carbon Analyzer (TOC-VCPN, Shimadzu, Japan). Total nitrogen (TN) was measured based on the absorption levels at 146 nm of water samples decomposed with alkaline potassium peroxydisulfate. Total phosphorus (TP) was determined using the molybdenum blue method after the samples were digested with potassium peroxydisulfate (APHA, 1998). pH was measured using a PHS-3C pH meter at room temperature (20±2℃).

2.2 CDOM absorption measurement

All water samples were filtered at low pressure at two steps: 1) filtered at low pressure through a pre-combusted Whatman GF/F filter (0.7μm), and 2) further filtered through pre-rinsed 25 mm Millipore membrane cellulose filter (0.22 μm). Absorption spectra were obtained between 200 and 800 nm at 1 nm increment using a Shimadzu UV-2600PC UV-Vis dual beam spectrophotometer (Shimadzu Inc., Japan) through a 1 cm quartz cuvette (or 5 cm cuvette for ice melted water samples). Milli-Q water was used as reference for CDOM absorption measurements. The Napierian absorption coefficient (a_{CDOM}) was calculated from the measured optical density (*OD*) of samples using Eq. (1):

$$a_{CDOM}(\lambda) = 2.303[OD_{S(\lambda)} - OD_{(null)}]/\beta \quad (1)$$

where β is the cuvette path length (0.01 or 0.05m) and 2.303 is the conversion factor of base 10 to base *e* logarithms. To remove the scattering effect from the limited fine particles remained in the filtered solutions, a necessitated correction was implemented by assuming the average optical density over 740–750 nm to be zero (Babin et al., 2003).

$SUVA_{254}$ and M values were calculated to characterize CDOM with respect to their compositional features. In addition, a_{CDOM} was divided into different groups according to M values by hierarchical cluster approach, which was performed in SPSS software package with the pairwise distance between samples was measured by squared Euclidean distance and the clusters were linked together by Ward's linkage method (Ward Jr, 1963). The method has been applied to classify the waters into different types according the remote sensing spectra (Vantrepotte et al., 2012; Shi et al., 2013).

3. Results

3.1. Water quality characteristics

Chl-a concentrations (46.44±59.71 μg/L) ranged from 0.28 to 521.12 μg/L. TN and TP concentrations were very high in fresh lakes, saline lakes and particularly urban water bodies (Table 1). It is worth noting that Chl-a concentration was still high 7.3±19.7 μg/L even in ice-covered lakes in winter from Northeast China. Electric conductivity (EC) and pH were high in the semi-arid and arid regions, and they were 1067-41000 μs/cm and 7.1-11.4, respectively. Overall, waters were highly turbid with high TSM concentrations (119.6 ± 131.4 mg/L), and apparent variations were observed for different types of waters (Table 1). Hydrographic conditions exerted strong impact on water turbidity and TSM concentration, thus these two parameters of river and stream samples were excluded in this study (Table 1).

[Insert Table 1 about here]

3.2. DOC concentrations in different types of waters

DOC concentrations changed remarkably in the investigated waters (Table 1). The concentration of DOC were low in rivers, and the lowest DOC concentrations were measured in ice melting waters. It should be noted that large variations were observed in water samples from rivers and streams (Table 2). Among the five types of waters, relatively higher DOC concentrations, ranging from 2.3 to 300.6 mg/L, were found in many saline lakes, in the Songnen Plain, the Hulunbuir Plateau and some areas in Tibetan Plateau (see Fig.2 for location). However, some of saline lakes supplied by snow melt water or ground water exhibited relatively lower DOC concentrations even with high salinity. Compared with samples collected in growing seasons, higher DOC concentrations (7.3-720 mg/L) were observed in ice-covered water bodies.

[Insert Table 2 about here]

3.3. DOC versus CDOM for various types of waters

3.3.1 Freshwater lakes and reservoirs

The relationship between DOC and CDOM has been investigated based on CDOM absorption at different wavelengths (Fichot and Benner, 2011; Spencer et al., 2012; Song et al., 2013; Brezonik et al., 2015). As suggested by Fichot and Benner (2011), CDOM absorptions at 275 nm ($a_{CDOM}(275)$) and 295 nm ($a_{CDOM}(295)$) have stable performances for DOC estimates for coastal waters. In current study, a strong relationship (R^2 = 0.85) between DOC and $a_{CDOM}(275)$ was found in fresh lakes and reservoirs (Fig.3a). However, the inclusion of $a_{CDOM}(295)$ explains very limited variance, thus it is not considered in the regression models. Regression analyses of water samples collected from different regions indicated that the slopes varied from 1.30 to 3.01 (Table 3). Water samples collected from East China and South China had lower regression slope values (Table 3), and lakes and reservoirs were generally mesotrophic or eutrophic (Huang et al., 2014; Yang et al., 2012, and references therein).

[Insert Table 3 about here]

[Insert Fig.3 about here]

3.3.2 Saline lakes

A strong relationship between DOC and $a_{CDOM}(275)$ (R^2 = 0.85) was demonstrated for saline lakes (Fig.3b) with much lower regression slope value (slope = 1.28). Further, the regression slopes exhibited large variations in different regions (Table 3), ranging from 0.86 in Tibetan waters to 2.83 in the Songnen Plain waters (see Fig.2 for location). As the extreme case, the slope value was only 0.33 as demonstrated in the embedded diagram in Fig.3b. Saline lakes in semi-arid or arid regions generally exhibit higher regression slope values, for example, the west Songnen Plain (2.83), the Hulunbir Plateau and the East Inner Mongolia Plateau (1.79). Whereas, waters in the west Inner Mongolia Plateau (1.13), the Tibetan Plateau (0.86) exhibited low slope values (Table 3), and the extreme low value was measured in the Lake Qinhai in Tibetan Plateau.

3.3.3 Streams and rivers

Although some of the samples scattered from the regression line (Fig.3c), close relationship between DOC and $a_{CDOM}(275)$ was found for samples collected in rivers and streams. Compared with the other water types (Fig.3), rivers and streams exhibited the highest regression slope value (slope = 3.01). Further regression analysis with water samples sub-datasets collected in different regions indicated that slope values presented large variability, ranging from 1.07 to 8.49. The lower regression slope values were recorded in water samples collected in rivers and stream in semi-arid and arid regions, such as the Tibetan Plateau, Mongolia Plateau and Tarim Basin, while the higher values were found in samples collected in streams originated from wetland and forest in Northeast China (Table 3).

To investigate the dynamics of CDOM absorption and DOC concentrations, three sections were investigated in three major rivers in Northeast China (see Figure S1 for location). River flow exerted obvious effect on DOC and CDOM (Fig.4) and flood impulse brought large amount of DOC and CDOM into river channels. The relationships between DOC and $a_{CDOM}(275)$ in sections along three rivers in Northeast China were demonstrated in Fig.5. The sampling point in the Yalu River is near the river head source, thus strong relationship (R^2=0.92) was exhibited with large slope (Fig.5a). The relationship between DOC and $a_{CDOM}(275)$ in the Songhua River at Harbin City section was much scattered (R^2=0.64, Fig.5c). With respect to Fig.5b, it is an in-between case (R^2=0.82). The sampling point was affected by effluent from Baishan City, thus the coefficient of determination (R^2= 0.822) and the regression slope (3.72) were lower than that from the Yalu River at Changbai point, while higher than that from the Songhua River at Harbin point.

[Insert Fig.4 and Fig.5 about here]

3.3.4 Urban waters

As shown in Fig.3d, relatively close relationship between DOC and $a_{CDOM}(275)$ was revealed in urban waters (R^2= 0.71, $p<0.001$). Similarly, regression slope values for urban waters also changed remarkably, ranging from 0.87 to 2.45 (Table 3). High nutrients in urban waters (Table 1) usually result in algal bloom in most urban water bodies (Chl-a range: 1.0-521.1μg/L; average: 38.9μg/L), which might contribute the high DOC concentrations in urban waters (Table 1). Thereby, the contribution from algal decomposition and cell lysis to DOC and CDOM should not be neglected for urban waters (Zhang et al., 2010; Zhao et al., 2016b; Zhou et al., 2016).

3.3.5 Ice covered lakes and reservoirs

The closest relationship (R^2 = 0.93) between DOC and $a_{CDOM}(275)$ was recorded in waters beneath ice covered lakes and reservoirs in Northeast China (Fig.3e). Comparatively, a weak relationship between DOC and $a_{CDOM}(275)$ was demonstrated in ice melting waters (Fig.3f). Apparently, CDOM from ice melting waters were mainly originated from maternal water during the ice formation, also from algal biological processes (Stedmon et al., 2011; Arrigo et al., 2010). Interestingly, the regression slopes for ice samples (1.35) and under lying water sample (1.27) are very close. In addition, there was a significant relationship between DOC in ice and underlying waters (R^2 = 0.86), indicating the dominant components of CDOM and DOC in the ice are from maternal underlying waters.

3.3.6 DOC versus $a_{CDOM}(440)$

CDOM absorption at 440 nm, i.e., $a_{CDOM}(440)$, is usually used as a surrogate to represent its concentration (Bricaud et al., 1981; Babin et al., 2003), and widely used in remote sensing community to quantify CDOM in waters (Lee et al., 2002; Binding et al., 2008; Zhu et al., 2014). Significant relationships between DOC and $a_{CDOM}(440)$ were found in different types of waters (Fig.5). Through comparing Fig.3 with Fig.6, it can be found that the overall relationships between DOC and CDOM at 440 nm resembled that at 275 nm for different types of waters, but with relatively loose relationship as indicated by the coefficients of determination (see Table S5). Further, it can be noted that some of the samples in Fig.3b-f and Fig.6b-f may leverage the regression model performances. Thus, regression models without these samples appearing to leverage the relationships were evaluated and provided in Table S6. Comparing Table S5 and Table S6, the regression model performances were degraded, but still acceptable.

[Insert Fig.6 about here]

3.4 CDOM molecular weight and aromacity versus DOC

3.4.1 CDOM versus $SUVA_{254}$ and M value ($a_{CDOM}(250)/a_{CDOM}(365)$)

The large slope variations of regressions between DOC and $a_{CDOM}(275)$ in different types of waters are probably due to the aromacity and colored fractions in DOC component (Spencer et al., 2009, 2012; Lee et al., 2015). As shown in Fig.7a, it can be seen that $SUVA_{254}$ had high values in fresh lakes, and waters from rivers or streams as well. Saline water and ice covered waters in Northeast China showed intermediate $SUVA_{254}$ values, while urban water and ice melting water exhibited lower values. The M value, i.e., $a_{CDOM}(250)/a_{CDOM}(365)$ is another indicator to demonstrate the variation of molecular weight of CDOM components (De Haan, 1993). Compared to saline water, fresh lake water (*t-Test*: $F = 631$, $p < 0.01$), river and stream water (*t-Test*: $F = 565$, $p < 0.001$), and urban water (*t-Test*: $F = 393$, $p < 0.001$) exhibited low M values (Fig.7b), which indicated that large weight molecules dominate in these three types of waters.

Saline water, ice covered water in Northeast China and ice melting water showed higher M values. Since $SUVA_{254}$ is a proxy based on the ratio to DOC, it is inappropriate to establish the relationship between CDOM and DOC based on the $SUVA_{254}$ classification. Thereby, only M values, which reveal molecular weight and aromacity, might help to estimate DOC through CDOM absorption based on M values for various types of waters.

[Insert Fig.7 about here]

3.4.2 Regression based on M values

Regression models between DOC and $a_{CDOM}(275)$ were established based on M value grouping. Four groups were achieved with hierarchical cluster approach, and each group occupied about 44.74% ($M < 9.0$), 34.24% ($9.0 < M < 16.0$), 18.22% ($16.0 < M < 25.0$) and 2.80% ($25.0 < M < 68.0$) of the total samples from group 1 to 4, respectively. Though only M values were used in the cluster which meant the feature space in classification only had one dimension and the groups were mainly divided according to the distribution of M values, the hierarchical cluster approach generated rational results. As shown in Fig.8, a close relationship ($R^2 = 0.90$) between DOC and $a_{CDOM}(275)$ was revealed in dataset where $M < 9.0$. Likewise, close relationship regression model appeared in dataset with intermediate M values (Group 2 in Fig.8), revealing high determination of coefficients ($R^2 = 0.91$). A relative weak relationship ($R^2 = 0.79$) between DOC and $a_{CDOM}(275)$ appeared with M values ranging from 16.0 to 25.0. A very close relationship ($R^2 = 0.98$) was found with extremely high M values (Group 4 in Fig.8).

As noted in Fig.8, close regression slopes implicated that a comprehensive regression model with intermediate M values less than 16 may be achieved. As expected, a promising regression model (the diagram was not shown) between DOC and $a_{CDOM}(275)$ was achieved ($y = 1.269x + 6.42$, $R^2 = 0.909$, $N = 1171$, $p < 0.001$) with pooled dataset in group 1 and group 2 shown in Fig.8. Inspired by this idea, the relationship between $a_{CDOM}(275)$ and DOC also examined with pooled data. As shown in Fig.9a, a significant relationship between DOC and $a_{CDOM}(275)$ was obtained with the pooled dataset (N = 1504) collected from different types of inland waters. However, it should be noted that the extremely high DOC samples may advantageously contribute the better performance of the regression model. Thus, regression model excluding these eight samples (DOC > 300 mg/L) was acceptable (Fig.9b, $R^2 = 0.51$, $p < 0.001$), but greatly degraded. In addition, regression model with power function was established in decimal logarithms log-log scale (Fig.9c, $R^2 = 0.77$, $p < 0.001$).

[Insert Fig.8 and Fig.9 about here]

4. Discussion

4.1 Variation of water quality parameters

Different water types were sampled across China with different climatic, hydrologic, and land use conditions in various catchment, combined with different anthropogenic intensity, thus the biological and geochemical properties in the water bodies are quite diverse with large range values for each parameters (Table 1). Extremely turbid waters are observed for fresh waters, saline waters and underlying waters covered by ice, which were generally collected in very shallow water bodies in different parts of China.

As expected, large variations of Chl-a are observed for both fresh waters and urban waters, and particularly these samples collected in urban waters show large range (1.0-521.1 μg/L). Our investigation also indicates that algal growth is still very active in these ice covered water bodies in Northeast China, which might result from high TN (4.3±5.4mg/L) and TP (0.7±0.6mg/L) concentrations in these waters bodies. It also should be noted that DOC, EC and pH were high in semi-arid or arid climatic regions, which are consistent with previous findings (Curtis and Adams, 1995; Song et al., 2013; Wen et al., 2016).

4.2 DOC variation with different types of waters

This investigation indicates that lower DOC were encountered with samples collected in rivers from the Tibetan Plateau (Table 2), where the average soil organic matter is lower, thus terrestrial DOC input from the catchment is less (Tian et al., 2008). However, high DOC concentrations were found in rivers or streams surrounded by forest or wetlands in Northeast China, the similar findings were also reported by Agren et al. (2007, 2011). Further, lower DOC concentration is also measured with ice samples, which is consistent with previous findings (Bezilie et al., 2002; Shao et al., 2016). But relatively high DOC concentration was observed for underlying waters covered by ice in Northeast China due to the condensed effect caused by the DOC discharged from ice formation (Bezilie et al., 2002; Shao et al., 2016; Zhao et al., 2016a). This condensed effect was particularly marked in these shallow water bodies where ice forming remarkably condensed the DOC in the underlying waters (Zhao et al., 2016a). It also should be noted that DOC concentration has a strong connection with hydrological condition and catchment landscape features (Neff et al., 2006; Agren et al., 2007; Lee et al., 2015). It should be noted that large DOC variations were observed in saline lakes in different regions (Table 2). Much higher DOC concentrations were found in saline lakes in Qinghai and Hulunbir, while relative low concentrations were observed in Xilinguole Plateau and the Songnen Plain, which is consistent with previous investigations conducted in the semi-arid or arid regions (Curtis and Adams, 1995; Song et al., 2013; Wen et al., 2016).

4.3 Variation of the relationships between CDOM and DOC

As demonstrated in Fig.3, obvious variation is revealed for the regression slope values between DOC and $a_{CDOM}(275)$. Most of the fresh water bodies are located in East China, where agricultural pollution and anthropogenic discharge have resulted in serious eutrophication (Tong et al., 2017). Phytoplankton degradation may contribute relative large portion of CDOM and DOC in these water bodies (Zhang et al., 2010; Zhou et al., 2016). Comparatively, fresh waters in Northeast and North China revealed larger regression slopes (Table 3). Waters in Northeast China are surrounded by forest, wetlands and grassland and therefore they generally exhibited high proportion of colored fractions of DOC. Further, soils in Northeast China are rich in organic carbon, which may also contribute to high concentration of DOC and CDOM in waters in this region (Jin et al., 2016; Zhao et al., 2016a). Compared with waters in East and South China, waters in Northeast China showed less algal bloom due to low temperature, thus autochthonous CDOM was less presented in waters in Northeast China (Song et al., 2013; Zhao et al., 2016a). As suggested by Brezonik et al. (2015) and Cardille et al.

(2013), CDOM in the eutrophic waters or those with very short resident time may show seasonal variation due to algal bloom or hydrological variability, while CDOM in some oligotrophic lakes or those with long resident time may show a stable pattern.

As shown in Fig.3b, smaller regression slope is revealed between DOC and $a_{CDOM}(275)$ for saline waters, indicating less colored portion of DOC was presented in waters in semi-arid to arid regions, especially for these closed lakes with enhanced photochemical processes, enhanced by longer residence time and strong solar radiation (Spencer et al., 2012; Song et al., 2013; Wen et al., 2016). The findings highlighted the difference for the relationship between CDOM and DOC, thus different regression models should be established to accurately estimate DOC in waters through linking with CDOM absorption, particularly for fresh and saline waters that showing different specific absorption coefficients (Song et al., 2013; Cardille et al., 2013; Brezonik et al., 2015).

DOC concentration is strongly associated with hydrological conditions (Neff et al. 2006; Agren et al. 2007; Yu et al., 2016). The relationships between CDOM and DOC in river and stream waters are very variable due to the hydrological variability and catchment features (Agren et al., 2011; Spencer et al., 2012; Ward et al., 2013; Lee et al., 2015; Zhao et al., 2017). As shown in Fig.4, the relationship between river flows and DOC is rather complicated, which is mainly caused by the land use, soil properties, relief, slope, the proportion of wetlands and forest, climate and hydrology of the catchments (Neff et al., 2006; Sobek et al., 2007; Spencer et al., 2012; Zhou et al., 2016), with additional influence by sewage discharge into rivers. The close relationship for head waters with higher regression slope value (Fig.5a) is mainly attributed to that the DOC and CDOM were fresh and less disturbed by pollution from anthropogenic activities (Spencer et al., 2012; Shao et al., 2016). However, both point and non-point source pollution complicated the relationship between DOC and DOM (Fig.5c).

4.4 Regression models based on CDOM grouping

As observed in Fig.3, the regression slopes (range: 0.33~3.01) for the relationship between DOC and $a_{CDOM}(275)$ varied significantly. The CDOM absorption coefficient is affected by its components and aromacity, thus the M values are used to classify CDOM into different groups, which turns to be an effective approach for improving regression models (Fig.8) between DOC and $a_{CDOM}(275)$. It also should be highlighted that the fourth group (Fig.8) is mainly from saline lakes (samples from embedded diagram in Fig.3b), thus the regression model slope is extremely low. From the regression model with pooled data, it can also be seen that relative accurate regression model for CDOM versus DOC can be achieved with data collected in inland waters at global scale (Sobek et al., 2007), which might be helpful in quantifying DOC through linking with CDOM absorption, and the latter parameter can be estimated from remote sensing data (Zhu et al., 2011; Kuster et al., 2015). Comparing Fig.8 and Fig.9b, it also should be noted that some of the saline waters with extremely low CDOM absorption efficiency (Group 4 in Fig.8) should be divided into different groups to achieve accurate DOC regression model through CDOM absorption.

5. Conclusions

Based on the measurement of CDOM absorption and DOC laboratory analysis, we have systematically examined the relationships between CDOM and DOC in various types of waters in China. This investigation showed that CDOM absorption varied significantly. River waters and fresh lake waters exhibited high CDOM absorption values and specific CDOM absorption ($SUVA_{254}$). On the contrast, saline lakes illustrated low $SUVA_{254}$ values probably due to the long residence time and strong photo-bleaching effects on waters in the semi-arid regions.

The current investigation indicated that the relationships between CDOM absorption and DOC varied remarkably by showing very varied regression slopes in various types of waters. Head river water generally exhibits larger regression slope values, while rivers affected by anthropogenic activities show lower slope values. Saline water generally reveals small regression slope due to the photobleaching effect in the semi-arid or arid region, combined with longer residence time. The accuracy of regression model between $a_{CDOM}(275)$ and DOC was improved when CDOM absorptions were divided into different sub-groups according to M values. Our finding highlights that remote sensing models for DOC estimation based on the relationship between CDOM and DOC should consider water types or cluster waters into several groups according to their absorption features.

Acknowledgements

The authors would like to thank financial supports from the National Key Research and

Development Project (No. 2016YFB0501502), Natural Science Foundation of China (No.41471290 and 41730104), and "One Hundred Talents" Program from Chinese Academy of Sciences granted to Dr. Kaishan Song. Thanks are also extended to all the staff and students for their efforts in field data collection and laboratory analysis, and Dr. Hong Yang to review and polish the English language. The authors are greatly indebted to associate Editor C. Stamm and these referees from both the previous and the current versions of the manuscript for their very valuable comments that greatly strengthened this manuscript.

References

Agren, A., Buffam, I., Jansson, M., Laudon, H., 2007. Importance of seasonality and small streams for the landscape regulation of dissolved organic carbon export. Journal of Geophysical Research, 112: G03003.

Agren, A., Haei, M., Kohler, S.J., Kohler, S.J., Bishop, K., Laudon, H., 2011. Regulation of stream water dissolved organic carbon (DOC) concentrations during snowmelt; the role of discharge, winter climate and memory effects. Biogeosciences, 7, 2901-2913.

APHA/AWWA/WEF. 1998. Standard methods for the examination of water and wastewater. Washington, DC: American Public Health Association.

Arrigo, K.R., Mock, T., Lizotte, M.P., 2010. Primary producers and sea ice, In *Sea Ice*, edited by D.N. Thomas, and G.S. Dieckmann, pp. 283-326, second ed., Wiley-Blackwell, Oxford, UK.

Babin, M., Stramski, D., Ferrari, G. M., Claustre, H., Bricaud, A., Obolensky, G., Hoepffner, N., 2003. Variations in the light absorption coefficients of phytoplankton, nonalgal particles, and dissolved organic matter in coastal waters around Europe. Journal of Geophysical Research, 108(C7), 3211.

Belzile, C., Gibson, J.A.E., Vincent, W.F., 2002. Colored dissolved organic matter and dissolved organic carbon exclusion from lake ice: implications for irradiance transmission and carbon cycling. Limnology and Oceanography, 47(5), 1283–1293.

Binding, C.E., Jerome, J.H., Bukata, R.P., Booty, W.G., 2008. Spectral absorption properties of dissolved and particulate matter in Lake Erie. Remote Sensing of Environment, 112(4), 1702-1711.

Brezonik, P.L., Olmanson, L.G., Finlay, J.C., Bauer, M.E., 2015. Factors affecting the measurement of CDOM by remote sensing of optically complex inland waters. Remote Sensing of Environment, 157, 199-215.

Bricaud, A., Morel, A., Prieur, L., 1981. Absorption by dissolved organic matter of the sea (yellow substance) in the UV and visible domains, Limnology and Oceanography, 26(1), 43– 53.

Cardille, J.A., Leguet, J.B., del Giorgio, P., 2013. Remote sensing of lake CDOM using noncontemporaneous field data. Canadian Journal of Remote Sensing, 39, 118–126.

Chen, R.F., Bissett, P., Coble, P., Conmy, R., Gardner, G.B., Moran, M.A., Wang, X.C., Wells, M.L., Whelan, P., Zepp, R.G., 2004. Chromophoric dissolved organic matter (CDOM) source characterization in the Louisiana Bight. Marine Chemistry, 89, 257-272.

Curtis, P.J., Adams, H.E., 1995. Dissolved organic matter quantity and quality from freshwater and saltwater lakes in east-central Alberta. Biogeochemistry 30, 59–76.

De Haan, H., 1993. Solar UV-light penetration and photodegradation of humic substances in peaty lake water. Limnology and Oceanography, 1993, 38, 1072–1076.

De Haan, H., De Boer, T., 1987. Applicability of light absorbance and fluorescence as measures of concentration and molecular size of dissolved organic carbon in humic Lake Tjeukemeer. Water Research, 21, 731–734.

Fichot, C.G., Benner, R., 2011. A novel method to estimate DOC concentrations from CDOM absorption coefficients in coastal waters. Geophysical Research Letter, 38, L03610.

Findlay, S.E.G., Sinsbaugh, R.L., 2003. Aquatic Ecosystems Interactivity of Dissolved Organic Matter. Academic Press, San Diego, CA, USA.

Gonnelli, M., Vestri, S., Santinelli, C., 2013. Chromophoric dissolved organic matter and microbial enzymatic activity. A biophysical approach to understand the marine carbon cycle. Biophysical Chemistry, 182, 79-85.

Helms, J.R., Stubbins, A., Ritchie, J.D., Minor, E.C., Kieber, D.J., Mopper, K., 2008. Absorption spectral slopes and slope ratios as indicators of molecular weight, source, and photobleaching of chromophoric dissolved organic matter. Limnology and Oceanography, 53, 955–969.

Huang, C.C., Li, Y.M., Yang, H., Li, J.S., Chen, X., Sun, D.Y., Le, C.F., Zou, J., Xu, L.J., 2014. Assessment of water constituents in highly turbid productive water by optimization bio-optical retrieval model after optical classification. Journal of Hydrology, 519, 1572–1583.

Jaffé, R., McKnight, D., Maie, N., Cory, R., McDowell, W.H., Campbell, J.L., 2008. Spatial and temporal variations in DOM composition in ecosystems: The importance of long-term monitoring of optical properties. Journal of Geophysical Research, 113, G04032.

Jeffrey, S.W., Humphrey G.F., 1975. New spectrophotometric equations for determining chlorophylls *a, b,* c_1, and c_2 in higher plants, algae and natural phytoplankton. Biochemie und Physiologie der Pflanzen, 167(2), 191–194.

Jin, X.L., Du, J., Liu, H.J., Wang, Z.M., Song, K.S., 2016. Remote estimation of soil organic matter content in the Sanjiang Plain, Northeast China: The optimal band algorithm versus the GRA-ANN model. Agricultural and Forest Meteorology, 218, 250–260.

Kowalczuk, P., Zablocka, M., Sagan, S., Kulinski, K., 2010. Fluorescence measured in situ as a proxy of CDOM absorption and DOC concentration in the Baltic Sea. Oceanologia, 52(3), 431–471.

Kutser, T., Verpoorter, C., Paavel, B., Tranvik, L.J., 2015. Estimating lake carbon fractions from remote sensing data. Remote Sensing of Environment, 157, 138–146.

Lai, L., Huang, X., Yang, H., Chuai, X., Zhang, M., Zhong, T., Chen, Z., Chen, Y., Wang, X., Thompson, J.R., 2016. Carbon emissions from land-use change and management in China between 1990 and 2010. Science Advances, 2(11), e1601063.

Le, C.F., Hu, C.M., Cannizzaro, J., Duan, H.T., 2013. Long-term distribution patterns of remotely sensed water quality parameters in Chesapeake Bay. Estuarine, Coastal and Shelf Science, 128(10), 93–103.

Lee, E.J., Yoo, G.Y., Jeong, Y., Kim, K.U., Park, J.H., Oh, N.H., 2015. Comparison of UV–VIS and FDOM sensors for in situ monitoring of stream DOC concentrations. Biogeosciences, 12, 3109–3118.

Lee, Z.P., Carder, K.L., Arnone, R.A., 2002. Deriving inherent optical properties from water color: A multiband quasi-analytical algorithm for optically deep waters. Applied Optics, 41(27), 5755–577.

Miller, W.L., Zepp, R.G., 1995. Photochemical production of dissolved inorganic carbon from terrestrial organic matter: Significance to the oceanic organic carbon cycle. Geophysical Research Letter, 22 (4), 417–420.

Neff, J.C., Finlay, J.C., Zimov, S.A., Davydov, S.P., Carrasco, J.J., Schuur, E.A.G., Davydova, A.I., 2006. Seasonal changes in the age and structure of dissolved organic carbon in Siberian rivers and streams. Geophysical Research Letter, 33, L23401.

Pekel, J.F., Cottam, A., Gorelick, N., Belward, A.S., 2016. High-resolution mapping of global surface water and its long-term changes. Nature, 540, 417–422.

Raymond, P. A., Hartmann, J., Lauerwarld, R., et al., 2013. Global carbon dioxide emissions from inland waters. Nature, 503(7476), 355–359.

Reche, I., Pace, M., Cole, J.J., 1999. Relationship of trophic and chemical conditions to photobleaching of dissolved organic matter in lake ecosystems. Biogeochemistry, 44, 529–280.

Shao, T.T., Song, K.S., Du, J., Zhao, Y., Ding, Z., Guan, Y., Liu, L., Zhang, B., 2016. Seasonal variations of CDOM optical properties in rivers across the Liaohe Delta. Wetlands, 36 (suppl.1): 181–192.

Shi, K., Li, Y., Li, L., et al., 2013. Remote chlorophyll-a estimates for inland waters based on a cluster-based classification. Science of the Total Environment, 444, 1–15.

Spencer, R.G.M., Stubbins, A., Hernes, P.J., Baker, A., Mopper, K., Aufdenkampe, A.K., Dyda, R.Y., Mwamba, V.L., Mangangu, A.M., Wabakanghanzi, J.N., Six, J., 2009. Photochemical degradation of dissolved organic matter and dissolved ligninphenols from the Congo River. Journal of Geophysical Research, 114, G03010.

Spencer, R.G.M., Butler, K.D., Aiken, G.R., 2012. Dissolved organic carbon and chromophoric dissolved organic matter properties of rivers in the USA. Journal of Geophysical Research, 117, G03001.

Sobek, S., Tranvik, L.J., Prairie, Y.T., Kortelainen, P., Cole, J.J., 2007. Patterns and regulation of dissolved organic carbon: An analysis of 7,500 widely distributed lakes. Limnology and Oceanography 52, 1208–1219.

Song, K.S., Zang, S.Y., Zhao, Y., Li, L., Du, J., Zhang, N.N., Wang, X.D., Shao, T.T., Liu, L., Guan, Y., 2013. Spatiotemporal characterization of dissolved Carbon for inland waters in semi-humid/semiarid region, China. Hydrology and Earth System Science, 17, 4269–4281.

Stedmon, C.A., Thomas, D.N., Papadimitriou, S., Granskog, M.A., Dieckmann, G.S. 2011. Using fluorescence to characterize dissolved organic matter in Antarctic sea ice brines. Journal of Geophysical Research, 116, G03027.

Tian, Y.Q., Ouyang, H., Xu, X.L., Song, M.H., Zhou, C.P., 2008. Distribution characteristics of soil organic carbon storage and density on the Qinghai-Tibet Plateau. Acta Pedologica Sinica, 45(5), 933–942. (In Chinese with English abstract).

Tong, Y.D., Zhang, W., Wang, X.J., et al., 2017. Decline in Chinese lake phosphorus concentration accompanied by shift in sources since 2006. Nature Geoscience, 10(7), 507–511.

Tranvik, L.J., Downing, J.A., Cotner, J.B., et al., 2009. Lakes and reservoirs as regulators of carbon cycling and climate. Limnology and Oceanography, 54(6), 2298–2314.

Vantrepotte, V., Loisel, H., Dessailly, D., et al., 2012. Optical classification of contrasted coastal waters. Remote Sensing of Environment, 123, 306–323.

Verpoorter, C., Kutser, T., Seekell, D.A., Tranvik, L.J., 2014. A global inventory of lakes based on high-resolutionsatellite imagery. Geophysical Research Letter, 41, 6396–6402.

Vodacek, A., Blough, N.V., Degrandpre, M.D., Peltzer, E.T., Nelson, R.K., 1997. Seasonal variation of CDOM and DOC in the Middle Atlantic Bight: terrestrial inputs and photooxidation. Limnology and Oceanography, 42, 674–686.

Ward Jr, J.H., 1963. Hierarchical grouping to optimize an objective function. Journal of the American Statistical Association, 58(301), 236–244.

Ward, N.D., Keil, R.G., Medeiros, P.M., Brito, D.C., Cunha, A.C., Dittmar, T., Yager, P.L., Krusche, A.V. and Richey, J.E., 2013. Degradation of terrestrially derived macromolecules in the Amazon River. Nature Geoscience, 6(7), 530–533.

Weishaar, J.L., Aiken, G.R., Bergamaschi, B.A., Fram, M.S., Fugii, R., Mopper, K., 2003. Evaluation of specific ultraviolet absorbance as an indicator of the chemical composition and reactivity of dissolved organic carbon. Environmental Science and Technology, 37, 4702–4708.

Wen, Z.D., Song, K.S., Zhao, Y., Du, J., Ma, J.H., 2016. Influence of environmental factors on spectral characteristic of chromophoric dissolved organic matter (CDOM) in Inner Mongolia Plateau, China. Hydrology and Earth System Sciences, 20, 787–801.

Williamson, C.E., Rose, K.C., 2010. When UV meets fresh water. Science, 329, 637–639.

Wilson, H., Xenopoulos, M.A., 2008. Ecosystem and seasonal control of stream dissolved organic carbon along a gradient of land use. Ecosystems 11, 555–568.

Yang, H., Andersen, T., Dörsch, P.,Tominaga, K., Thrane, J.-E., Hessen, D. O., 2015. Greenhouse gas metabolism in Nordic boreal lakes. Biogeochemistry, 126, 211–

225.
Yang, H., Xie, P., Ni, L., Flower, R. J., 2012. Pollution in the Yangtze. Science, 337, (6093), 410-410.
Yu, Q., Tian, Y, Q., Chen, R.F., Liu, A., Gardner, G.B., Zhu, W.N., 2010. Functional linear analysis of in situ hyperspectral data for assessing CDOM in rivers. Photogrammetric Engineering＆Remote Sensing, 76(10), 1147–1158.
Yu, X.L., Shen, F., Liu, Y.Y., 2016. Light absorption properties of CDOM in the Changjiang (Yangtze) estuarine and coastal waters: An alternative approach for DOC estimation. Estuarine, Coastal and Shelf Science, 181, 302–311.
Zhang, Y.L., Zhang, E.L., Yin, Y., Van Dijk, M.A., Feng, L.Q., Shi, Z.Q., Liu, M.L., Qin, B.Q., 2010. Characteristics and sources of chromophoric dissolved organic matter in lakes of the Yungui Plateau, China, differing in trophic state and altitude. Limnology and Oceanography, 55(6), 2645–2659.
Zhao, Y., Song, K.S., Wen, Z.D., Li, L., Zang, S.Y., Shao, T.T., Li, S.J., Du, J., 2016a. Seasonal characterization of CDOM for lakes in semiarid regions of Northeast China using excitation–emission matrix fluorescence and parallel factor analysis (EEM－PARAFAC). Biogeosciences, 13, 1635–1645.
Zhao, Y., Song, K.S., Li, S.J., Ma, J.H., Wen, Z.D., 2016b. Characterization of CDOM from urban waters in Northern-Northeastern China using excitation-emission matrix fluorescence and parallel factor analysis. Environmental Science and Pollution Research, 23, 15381–15394.
Zhao, Y., Song, K.S., Shang, Y. X., Shao, T. T., Wen, Z.D., Lv, L.L., 2017.

Characterization of CDOM of river waters in China using fluorescence excitation-emission matrix and regional integration techniques. Journal of Geophysical Research, Biogeoscience, DOI: 10.1002/2017JG003820.

Zhou Y., Zhang Y., Jeppesen E., Murphy K.R., Shi K., Liu M., Liu X., Zhu G. Inflow rate-driven changes in the composition and dynamics of chromophoric dissolved organic matter in a large drinking water lake. Water Research, 2016, 100, 211-221.

Zhu, W., Yu, Q., Tian, Y. Q., Chen, R.F., Gardner, G.B., 2011. Estimation of chromophoric dissolved organic matter in the Mississippi and Atchafalaya river plume regions using above-surface hyperspectral remote sensing. Journal of Geophysical Research: Oceans (1978–2012), 116(C2), C02011.

Zhu, W.N., Yu, Q., Tian, Y. Q., et al., 2014. An assessment of remote sensing algorithms for colored dissolved organic matter in complex freshwater environments. Remote Sensing of Environment, 140, 766-778.

Figures

Fig.1. The potential regulating factors that influence the relationship between CDOM and DOC. Note, CDOM sources are a subset of DOC sources, and hydrological feature includes flow discharge, drainage area, catchment landscape, river level, and inflow or outflow regions.

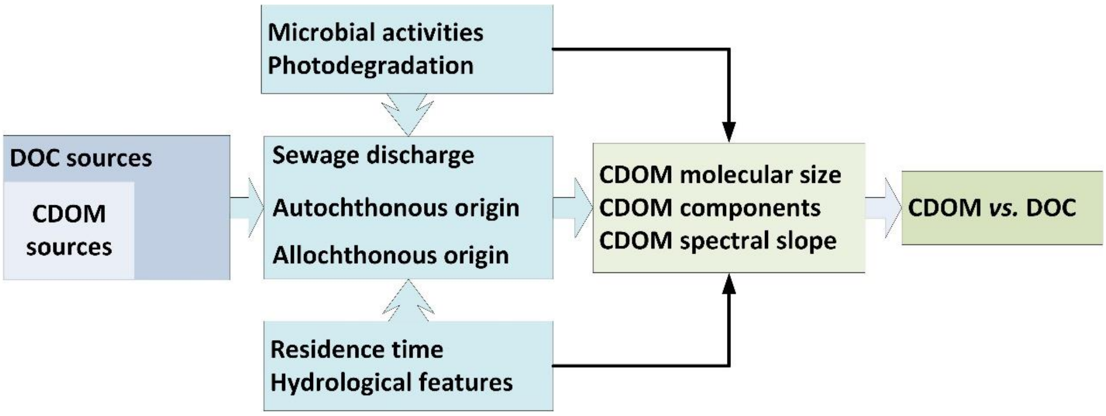

Fig.2. Water types and sample distributions across the mainland China. The dash line shows the boundary of some typical geographic units (i.e., Songnen Plain, and Hulunbuir Plateau).

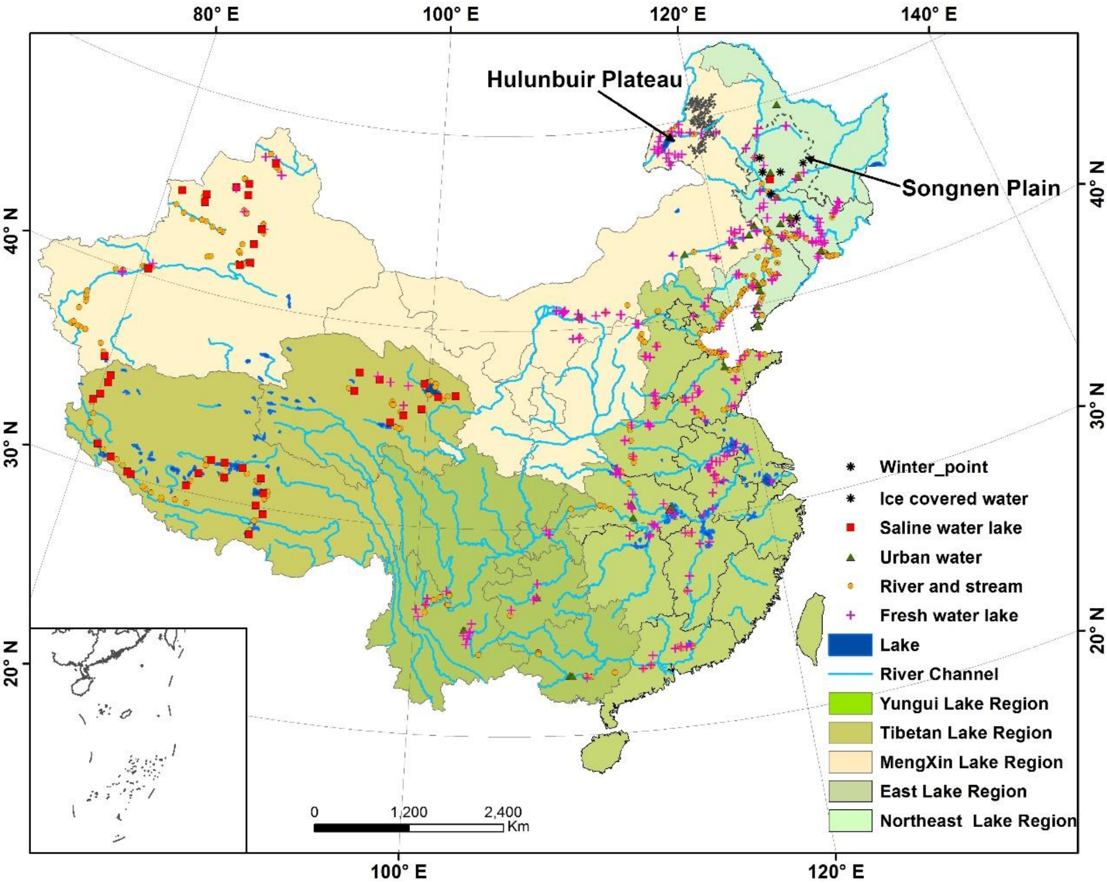

Fig.3. Relationship between DOC and $a_{CDOM}(275)$ in different types of inland waters, (a) fresh water lakes, (b) saline water lakes, (c) river and stream waters, (d) urban waters, (e) ice covered lake underlying waters, and (f) ice melting lake waters. The regression metrics without these high DOC concentrations in Fig.3b-f were listed in Tables S6.

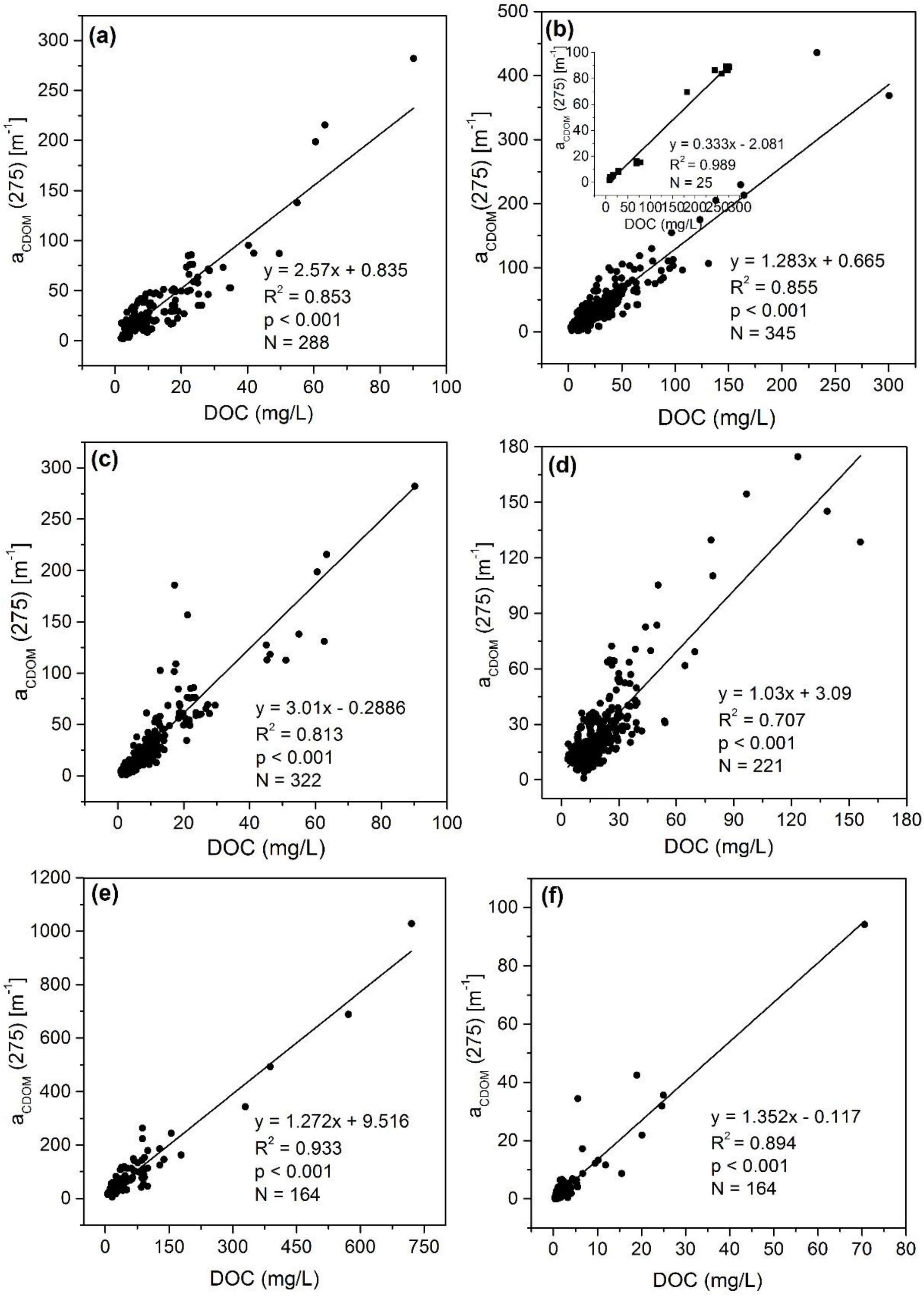

Fig.4. Concurrent flow dynamics for three rivers in Northeast China and the corresponding DOC and CDOM variations in 2015; (a) the Yalu River near Changbai County, (b) the Hunjiang River with DOC and CDOM sampled at Baishan City, while the river flow gauge station is near the Tonghua City, (c) the Songhua River at Harbin City.

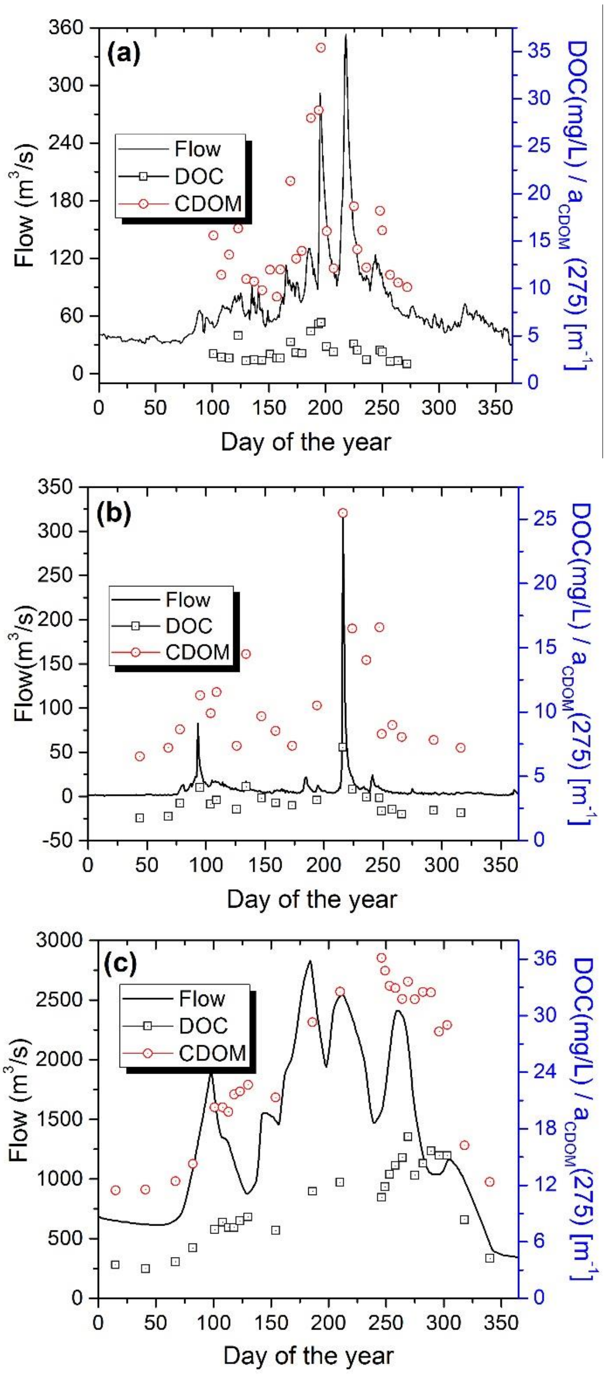

Fig.5. The relationships between $a_{CDOM}(275)$ and DOC at sections across (a) the Yalu River, (b) the Hunjiang River, and (c) the Songhua River. The samples were collected at each station at about one week or around ten days in ice free season in 2015.

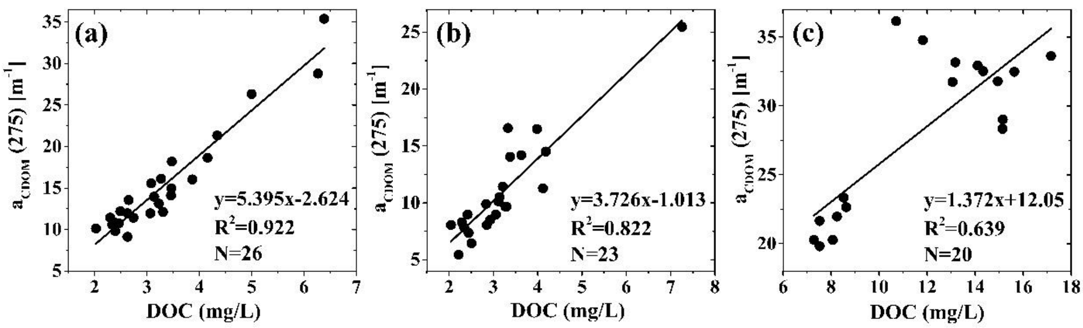

Fig.6. Relationship between DOC and $a_{CDOM}(440)$ in different types of inland waters, (a) fresh water lakes, (b) saline water lakes, (c) river and stream waters, (d) urban waters, (e) ice covered lake underlying waters, and (f) ice melting waters. The regression metrics without these high DOC concentrations in Fig.6b-f were listed in Tables S6.

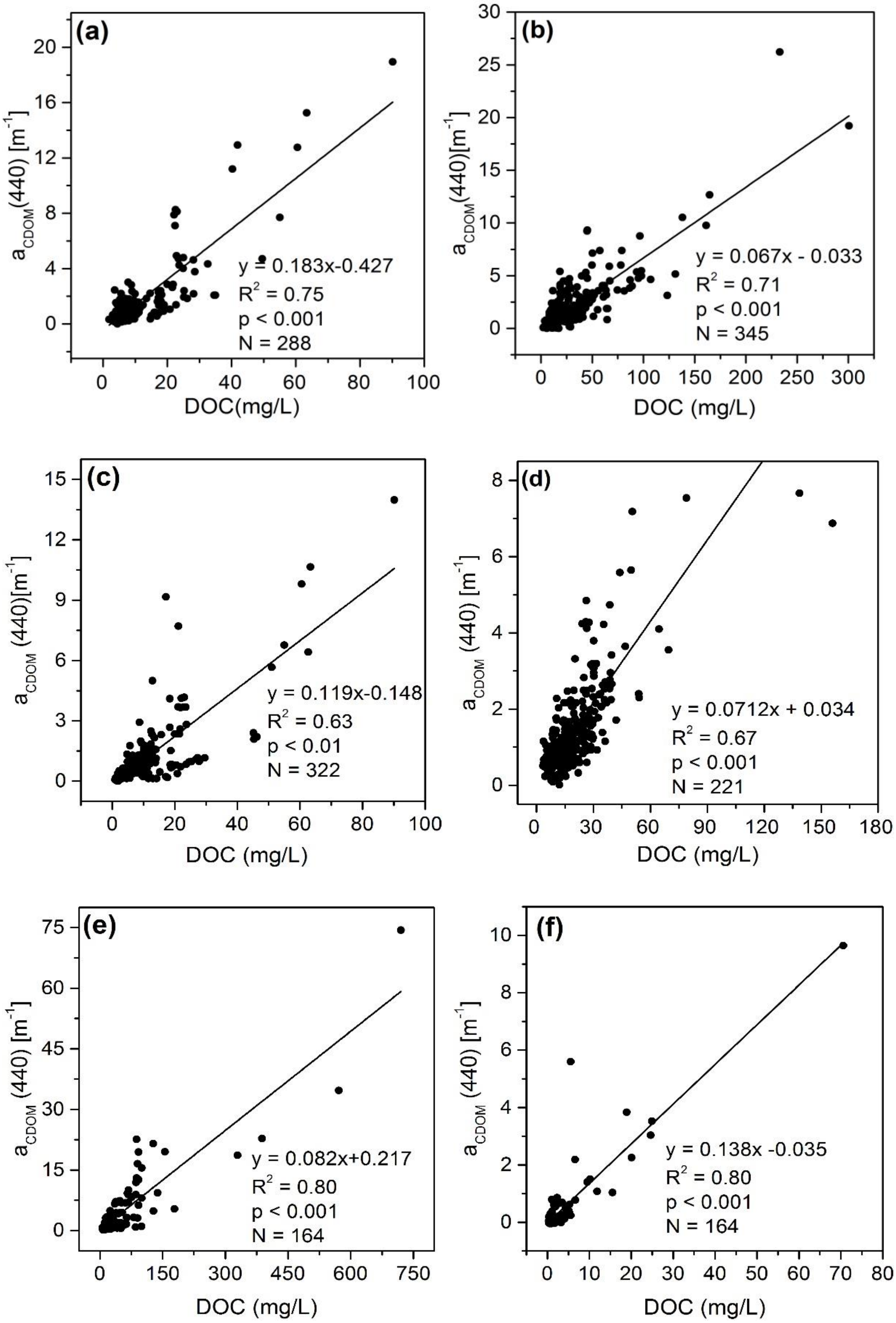

Fig.7. Comparison of (a) $SUVA_{254}$, and (b) M values ($a_{CDOM}(250)$ / $a_{CDOM}(365)$) in various types of inland waters. FW, fresh lake water; SW, saline lake water, RW, river or stream water; UW, urban water; WW, ice covered waters from Northeast China; IMW, ice melt waters from Northeast China.

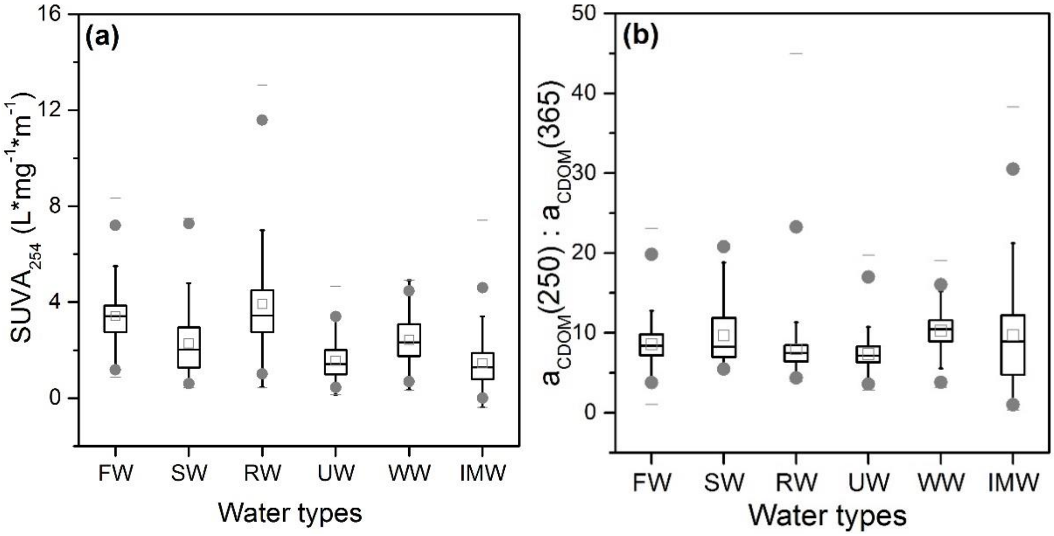

Fig.8. Relationship between DOC and $a_{CDOM}275$ sorted by M ($a_{CDOM}(250)/a_{CDOM}(365)$) values, Group 1: M <9.0; Group 2: 9.0< M<16.0; Group 3: 16.0< M< 25.0; Group 4: 25.0< M< 68.0.

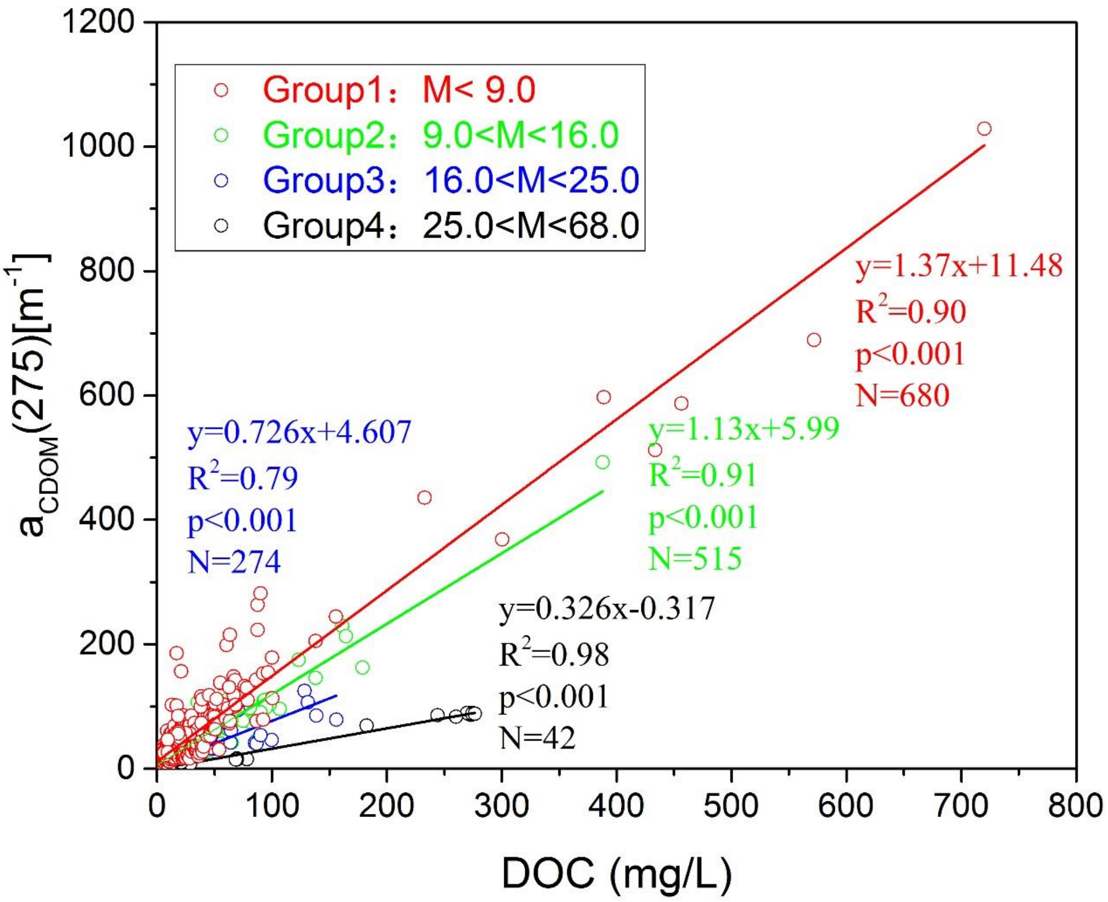

Fig.9. the relationships between $a_{CDOM}(275)$ and DOC concentrations, (a) regression model with pooled dataset; (b) regression model with DOC concentration less than 300 mg/L; (c) regression model with power fitting function based on log-log scale.

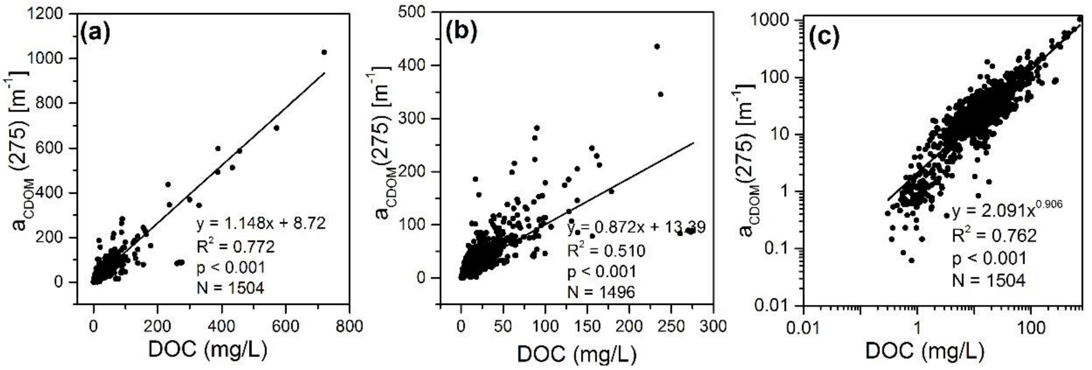

Tables

Table 1. Water quality in different types of waters, DOC, dissolved organic carbon; EC, electrical conductivity; TP, total phosphorus; TN, total nitrogen; TSM, total suspended matter; Chl-a, chlorophyll-a concentration.

		DOC (mg/L)	EC μs/cm	pH	TP (mg/L)	TN (mg/L)	TSM (mg/L)	Chl-a (μg/L)
FW	Mean	10.2	434.0	8.2	0.5	1.6	67.8	78.5
	Range	1.9-90.2	72.7-1181.5	6.9-9.3	0.01-10.4	0.001-9.5	0-1615	1.4-338.5
SW	Mean	27.3	4109.4	8.6	0.4	1.4	115.7	9.0
	Range	2.3-300.6	1067-41000	7.1-11.4	0.01-6.3	0.6-11.0	1.4-2188	0-113.7
RW	Mean	8.3	10489.1	7.8-9.5	-	-	-	-
	Range	0.9-90.2	3.7-1000	8.6	-	-	-	-
UW	Mean	19.44	525.4	8.0	3.4	3.5	50.5	38.9
	Range	3.5-123.3	28.6-1525	6.4-9.2	0.03-32.4	0.04-41.9	1-688	1.0-521.1
WW	Mean	67.0	1387.6	8.1	0.7	4.3	181.5	7.3
	Range	7.3-720	139-15080	7.0-9.7	0.1-4.8	0.5-48	9.0-2174	1.0-159.4
IMW	Mean	6.7	242.8	8.3	0.19	1.1	17.4	1.1
	Range	0.3-76.5	1.5-4350	6.7-10	0.02-2.9	0.3-8.6	0.3-254.6	0.28-5.8

Note: FW, fresh water lake; SW, saline water lake, RW, river or stream water; UW, urban water; WW, ice covered winter water from Northeast China; IMW, ice melt water from Northeast China.

Table 2. Descriptive statistics of dissolved organic carbon (DOC) and $a_{CDOM}(440)$ in various types of waters. Min, minimum; Max, maximum; S.D, standard deviation.

Type	Region	DOC (mg/L)				$a_{CDOM}(440)$ [m^{-1}]			
		Min	Max	Mean	S.D	Min	Max	Mean	S.D
River	Liaohe	3.6	48.2	14.3	9.49	0.46	3.68	0.92	0.58
	Qinghai	1.2	8.5	4.4	1.96	0.13	2.11	0.54	0.63
	Inner Mongolia	16.9	90.2	40.4	24.84	0.32	7.46	1.03	2.11
	Songhua	0.9	21.1	8.1	4.96	0.32	18.93	3.2	4.19
Saline	Qinghai	1.7	130.9	67.9	56.7	0.13	0.86	0.36	0.23
	Hulunbir	8.4	300.6	68.5	69.2	0.82	26.21	4.41	4.45
	Xilinguole	3.74	45.4	14.2	8.8	0.36	4.7	1.34	0.88
	Songnen	3.6	32.6	16.4	7.4	0.46	33.80	2.4	3.78

Table 3. Fitting equations for DOC against $a_{CDOM}(275)$ in different types of waters except ice covered lake underlying water and ice melting waters.

Water types	Region or Basin	Equations	R^2	N
Freshwater lakes	Northeast Lake Region	y = 3.13x-3.438	0.87	102
	MengXin Lake Region	y = 2.16x-1.279	0.90	63
	East Lake Region	y = 1.98x+7.813	0.66	69
	Yungui Lake Region	y = 1.295x-44.56	0.71	54
Saline lakes	Songnen Plain	y = 2.383x+1.101	0.92	159
	East Mongolia	y = 1.791x+8.560	0.67	57
	West Mongolia	y = 1.133x+3.900	0.81	46
	Tibetan Lake Region	y = 0.864x+2.255	0.84	83
Rivers or streams	Branch of the Nenjiang River	y = 7.655x-42.64	0.81	33
	Songhua River stem	y = 3.759x-6.618	0.71	29
	Branch of Songhua River	y = 8.496x-12.14	0.98	33
	Liao River Autumn 2012	y = 1.099x+3.900	0.80	38
	Liao River Autumn 2013	y = 1.073x-4.157	0.88	28
	Rivers from North China	y = 3.154x-1.207	0.87	48
	Rivers from East China	y = 3.037x-2.585	0.88	47
	Rivers from Tibetan Plateau	y = 2.345x+2.375	0.87	41
Urban waters	Waters from Changchun	y = 2.471x-2.231	0.54	48
	Waters from Harbin	y = 1.413x-4.521	0.67	31
	Waters from Beijing	y = 0.874x+11.12	0.63	27
	Waters from Tianjin	y = 0.994x + 7.368	0.57	23